Title
THERMODYNAMICS OF Na2SO4-INDUCED HOT CORROSION

Authors
Misra, A.K.
Whittle, D.P.
Worrell, W.L.

Publication Date
1981-10-01

LBL-13561 c.2
Preprint

Lawrence Berkeley Laboratory
UNIVERSITY OF CALIFORNIA

Materials & Molecular Research Division

Submitted to the Journal of the Electrochemical Society

THERMODYNAMICS OF Na_2SO_4-INDUCED HOT CORROSION

A.K. Misra, D.P. Whittle, and W.L. Worrell

October 1981

Prepared for the U.S. Department of Energy under Contract W-7405-ENG-48

THERMODYNAMICS OF Na_2SO_4-INDUCED HOT CORROSION

A. K. Misra and D. P. Whittle*

Lawrence Berkeley Laboratory
and
Department of Materials Science and Mineral Engineering
University of California
Berkeley, CA. 94720

W. L. Worrell*

Department of Metallurgy
University of Pennsylvania
Philadelphia, PA.

*Electrochemical Society Active Member

Keywords: Alloys, Corrosion, Thermodynamics

This work was supported by the Director, Office of Energy Research, Office of Basic Energy Sciences, Materials Science Division of the U.S. Department of Energy under Contract Number W-7405-ENG-48.

ABSTRACT

Quantitative studies of the formation of low melting point sulfates were made by equilibrating NiO-Na_2SO_4 mixtures with argon-SO_2-SO_3-air mixtures of different compositions in the temperature range 1000-1173K. Using these data and the Na_2SO_4 phase diagram, the enthalphy of fusion and melting temperature of $NiSO_4$ were estimated. The free energy of fusion of $NiSO_4$ is given by

$$\Delta G° = -40695 + 36.95\ T\ \text{cal.}$$

This has then been used to calculate the minimum P_{SO_3} required for liquid sulfate formation. Similar calculations were carried out from existing data for the $CoSO_4$-Na_2SO_4 system, and verified by a limited number of experiments. The minimum P_{SO_3} required for liquid sulfate formation is approximately an order of magnitude lower for Co-base alloys compared with Ni-base alloys, and the implications of this with regard to hot corrosion are discussed.

1. INTRODUCTION

The hot corrosion of blades and first-stage guide vanes of gas turbines exposed to marine and industrial atmospheres has received considerable attention in the recent past. The accelerated oxidation or hot corrosion is primarily due to a deposit of Na_2SO_4 on the blade surface and depending on the temperature, the deposit is either molten or solid. (The melting point of pure Na_2SO_4 is 884°C.) In addition to the Na_2SO_4 deposit, however, the atmosphere within the gas turbine engine always contains oxides of sulfur, SO_2 and SO_3, as a result of sulfur impurities in the fuel. The SO_3/SO_2 ratio depends on temperature and is higher at lower temperatures.

Goebel and Pettit (1) have described a fluxing mechanism for the accelerated corrosion of metals and alloys in the presence of molten Na_2SO_4, in which the protective oxides are dissolved in the Na_2SO_4 melt and, depending on the Na_2O activity in the melt, this dissolution is either by a basic or by an acidic fluxing mechanism. The acidic fluxing mechanism primarily involves dissolution of metal oxides as sulfates, and can be described by the reaction:

$$MO(s) + Na_2SO_4(l) = \underline{MSO_4}(l)(\text{dissolved in } Na_2SO_4) + Na_2O \qquad (1)$$

In contrast to hot corrosion above 900°C, where Na_2SO_4 is molten and the corrosion proceeds by the interaction of metal oxides with the Na_2SO_4 melt directly, low temperature (650-850°C) corrosion requires the formation of low melting mixed sulfates (2-5) by the reaction of metal oxides with SO_3 in the atmosphere via the reaction:

$$MO(s) + SO_3(g) = \underline{MSO_4}(l)(\text{dissolved in } Na_2SO_4) \qquad (2)$$

which is similar to that of acidic fluxing.

As is evident from reactions (1) and (2), prediction of the corrosion behavior of alloys requires a knowledge of the thermodynamic properties of the molten mixed sulfates and the systems of interest include Na_2SO_4-$CoSO_4$, Na_2SO_4-$NiSO_4$, Na_2SO_4-$Fe_2(SO_4)_3$, Na_2SO_4-$Cr_2(SO_4)_3$ and Na_2SO_4-$Al_2(SO_4)_3$, since alloys or coatings based on Fe, Ni, or Co alloyed with Cr and/or Al are widely used for hot corrosion resistance. The standard Gibbs free energy changes for reactions (1) and (2) are not available, since there are no data for the Gibbs free energy of formation of the various liquid metal sulfates (e.g. $CoSO_4$ $NiSO_4$), $Fe_2(SO_4)_3$, $Al_2(SO_4)_3$ and $Cr_2(SO_4)_3$). In addition, the partial molar properties of the mixed sulfates have received little attention and the only available data are solubilities of NiO, Co_3O_4(6), Al_2O_3(7) and Cr_2O_3(7, 8) in molten Na_2SO_4 as a function of Na_2O activity at 1200 K, in the very dilute solution range.

The partial molar properties of the molten mixed sulfates can also be estimated from an analysis of the existing binary Na_2SO_4-MSO_4 or Na_2SO_4-$M_2(SO_4)_3$ phase diagrams (9). However, as indicated earlier, estimation of the SO_3 pressure required to form the liquid sulfate mixture and hence a rationalization of the corrosion behavior, also requires melting point and entropy (or enthalphy) of fusion data for the metal sulfates. These are only available for $CoSO_4$(10) and Luthra and Shores (4, 5) have used these to analyze the corrosion behavior of Co and Co-base alloys in the temperature range 600-900°C. Using the Na_2SO_4-$CoSO_4$ phase diagram, they estimated a negative deviation from ideality in the molten sulfate. However, their analysis was based on the assumption that the melt consists of molecular species, Na_2SO_4 and $CoSO_4$, whereas in reality the molten salt is ionic and must be treated as a random solution of Na^+ and Co^{++} ions. In addition, their estimation of the Gibb's free energy data for $CoSO_4$(l) was based on the melting point (10) and an estimated entropy of melting of 3.5 cal. K^{-1} g. $mole^{-1}$ or 1.75 cal. K^{-1} g. ion^{-1}. Comparison with entropies of fusion (enthalpy of fusion ÷ melting temperature) for other MSO_4 sulfates (Table I) shows that generally these are somewhat greater than their estimate.

Thus, there is clearly a need for further analysis of the Na_2SO_4-$CoSO_4$ system, and a better estimation of the entropy of fusion of $CoSO_4$, in order to be able to predict the thermodynamic properties of the Na_2SO_4-$CoSO_4$ melt.

Unfortunately, for other sulfates of interest in hot corrosion, (e.g., $NiSO_4$, $Fe_2(SO_4)_3$, $Al_2(SO_4)_3$ and $Cr_2(SO_4)_3$) melting point data are not available, and the Gibbs free energy of formation of the liquid sulfates must be determined experimentally.

As a part of a larger program, aimed at deriving the thermodynamic properties of the molten mixed sulfates of importance to hot corrosion, the present paper is concerned with: (1) determination of the partial molar properties of the Na_2SO_4-$CoSO_4$ system from an analysis of the binary phase diagram and estimation of the free energy data for $CoSO_4$(l), with limited experimental verification, and (2) experimental determination of the Gibbs free energy of formation of $NiSO_4$(l) and the partial molar properties of the Na_2SO_4-$NiSO_4$ melt, using a gas-equilibration technique. The relevance of these analyses and measurements to hot corrosion phenomena are also discussed. The philosophy behind the work has been to extract as much information as possible from existing phase diagram data.

2. THEORETICAL CONSIDERATIONS

The molten salt mixtures considered in this paper are of the Na_2SO_4-MSO_4 type and can be treated as mixtures of Na^+, M^{++} and $SO_4^=$ ions. Thus, the salt mixture consists of cations of different charges, for which Forland (11) has given a general thermodynamic description. Assuming a random distribution of cations (Na^+ and M^{++}), i.e. Temkin mixing, the partial molar entropies of Na_2SO_4 and MSO_4 in the melt, $\overline{S}_{Na_2SO_4}$ and $\overline{S}_{MSO_4}$ respectively, can be described by

$$\bar{S}_{Na_2SO_4} = -R \ln(N_{Na^+})^2 \text{ and } \bar{S}_{MSO_4} = -R \ln (N_{M^{++}}) \qquad (3)$$

N_{Na^+} and $N_{M^{++}}$ are the cation fractions in the melt, and from mass balance consideration are given by

$$N_{Na^+} = \frac{2x_{Na_2SO_4}}{1+x_{Na_2SO_4}} \quad \text{and} \quad N_{M^{++}} = \frac{x_{MSO_4}}{1+x_{Na_2SO_4}} \qquad (4)$$

where $x_{Na_2SO_4}$ and x_{MSO_4} are the mole fractions of Na_2SO_4 and MSO_4 in the melt.

In order to obtain the partial molar enthalpies of the components, an equivalent cation fraction approach must be used to take into account differences in charge between the cations. Accordingly,

$$N'_{Na^+} = x_{Na_2SO_4} \qquad \text{and} \qquad N'_{M^{++}} = x_{MSO_4} \qquad (5)$$

where N'_{Na} and $N'_{M^{++}}$ are the respective equivalent ionic fractions. Then, combining this with a regular solution approximation, which is frequently used in liquid melts (9), the partial molar enthalpies of the components, $\bar{H}_{Na_2SO_4}$ and $\bar{H}_{MSO_4}$, in the Na_2SO_4-MSO_4 melt are given by

$$\bar{H}_{Na_2SO_4} = \omega_L (1-x^L_{Na_2SO_4})^2 \text{ and } \bar{H}_{MSO_4} = \omega_L (1-x^L_{MSO_4})^2 \qquad (6)$$

ω_L is an interaction energy parameter which is assumed to be independent of temperature and composition. Combining together eqns.(3), (4) and (6) gives the activities in the molten sulfate melt:

$$\ln a^L_{Na_2SO_4} = \ln \left\{ \frac{2x^L_{Na_2SO_4}}{1+x^L_{Na_2SO_4}} \right\}^2 + \frac{\omega_L}{RT} (1-x^L_{Na_2SO_4})^2 \qquad (7)$$

$$\ln a^L_{MSO_4} = \ln \left\{ \frac{x^L_{MSO_4}}{1+x^L_{Na_2SO_4}} \right\} + \frac{\omega_L}{RT} (1-x^L_{MSO_4})^2 \qquad (7)$$

3. ANALYSIS OF THE Na_2SO_4-$CoSO_4$ PHASE DIAGRAM

The Na_2SO_4-$CoSO_4$ phase diagram (12) is shown in Figure 1. The $CoSO_4$-rich side of the diagram is not well established. The Na_2SO_4-rich side shows a terminal solid solution. Thus, at any temperature, Na_2SO_4 in solid solution is in equilibrium with the Na_2SO_4 in the melt, and for the solid-liquid equilibrium,

$$\underline{Na_2SO_4}(s) \rightarrow \underline{Na_2SO_4}(l) \qquad (8)$$

$$\Delta G^\circ_{fusion}\ (Na_2SO_4) = -RT\ln \frac{a^L_{Na_2SO_4}}{a^S_{Na_2SO_4}} \qquad (9)$$

The standard Gibbs free energy of fusion of Na_2SO_4 at temperatures other than the melting point (884°C) is obtained from the expression:

$$\Delta G^\circ_{fusion}(Na_2SO_4) = \int_{T_M}^{T} \Delta c_p dT - T\int_{T_M}^{T} \Delta c_p d\ln T \qquad (10)$$

where T_M is the melting point and Δc_p the difference in heat capacity between liquid and solid Na_2SO_4. The heat capacity of $Na_2SO_4(l)$ was assumed to be constant, and an expression for that of the solid was obtained from Barin and Knacke (10). The activity of Na_2SO_4 in the melt can be described by eqn.(7). The solid solution, can be approximated to a dilute solution, when the solvent, Na_2SO_4, approximates to Raoultian behavior. Thus, again using the Temkin model for this ionic solid (13) gives

$$a^S_{Na_2SO_4} = \left\{\frac{2x^S_{Na_2SO_4}}{1+x^S_{Na_2SO_4}}\right\}^2 \qquad (11)$$

Combining eqns.(7),(9) and (11) and using the liquidus and solidus data from the phase diagram, allow the interaction parameter for the liquid sulfate melt, ω_L, to be calculated. Values calculated at different temperatures are shown in Table II. According to the model, ω_L should, of course, be constant. However, there is no systematic variation with temperature, and an average value of -6.2 ± 2 kcal. mole^{-1} has been adopted. Use of this average value to recalculate the liquidus curve shows close agreement with the original phase diagram.

4. ESTIMATION OF THE ENTHALPY AND ENTROPY OF FUSION OF $CoSO_4$

Since the melting point of $CoSO_4$(1266K) is known (10), the enthalpy of fusion can be obtained from an estimate of the entropy of fusion ($\Delta H^\circ_{fusion} = T_M \Delta S^\circ_{fusion}$), based on the entropies of fusion of other sulfates of the MSO_4-type (Table I). However, it appears that these data were estimated by Kelley (14) and were based on enthalpies of fusion obtained from freezing point lowering data. Unfortunately, Kelley failed to recognize the ionic nature of the molten salts in his analysis. As a consequence, it has been necessary to recalculate the enthalpies of fusion and hence the entropies. In addition, data (melting points and phase diagrams) for two other sulfates, $CdSO_4$ (15) and $CuSO_4$ (16) are now available.

Thus, on the MSO_4-rich side of the binary MSO_4-N_2SO_4 (N = Li, Na or K) diagram, if there is no terminal solid solution, the solid-liquid equilibrium is described by

$$MSO_4(s) = \underline{MSO_4}(l) \tag{12}$$

and the standard Gibb's free energy of fusion is given by

$$\Delta G^\circ_{fusion(MSO_4)} = -RT\ln a^L_{MSO_4} \tag{13}$$

The free energy and enthalpy of fusion are of course interrelated through

$$\frac{\partial(\Delta G^\circ_{fusion}/T)}{\partial\ (1/T)} = \Delta H^\circ_{fusion} = -R\,\frac{\partial \ln a^L_{MSO_4}}{\partial\ (1/T)} \tag{14}$$

Using the ionic model for the molten salt melt, and assuming that in the dilute solution range Temkin mixing is ideal, the activity of MSO_4 in the melt is given by

$$a^{L}_{MSO_4} = \left\{ \frac{x_{MSO_4}}{1+x_{N_2SO_4}} \right\} \qquad (15)$$

Thus, a plot of $\ln \frac{x_{MSO_4}}{1+x_{N_2SO_4}}$ versus (1/T) should be linear, with a slope of $-\Delta H_{fusion(MSO_4)}/R$. Departure from this linear relationship at higher solute (N_2SO_4) concentrations are due to deviations from ideal behavior. Table III summarises the estimated enthalpies and entropies of fusion, comparing the former values with the original estimates of Kelley (14); Kelley's estimated entropies were given in Table I.

The assumption, in this work, of an ionic model for the salt melt gives $\Delta H^{\circ}_{fusion}$ values slightly higher than those of Kelley (14) and as a consequence an average value for $\Delta S^{\circ}_{fusion}$ for sulfates of the MSO_4-type appears to be approximately 3 cal K^{-1}g. ion^{-1}. Kubaschewski et.al.(24) have also suggested an approximate value of 3 cal. K^{-1} g. ion^{-1} for ionic compounds of this type. Thus, based on this value and the melting point of 1266K, the enthalpy of fusion for $CoSO_4$ is estimated as 7.6 K cal. $mole^{-1}$.

5. Na_2SO_4 - $NiSO_4$ SYSTEM

The melting point of $NiSO_4$ is not available, and thus the Gibb's free energy of formation of $NiSO_4$(l) has to be determined experimentally. Thus, using a gas equilibration technique, the equilibrium $NiSO_4$ content of a Na_2SO_4-$NiSO_4$ melt was measured as a function of temperature and SO_3 partial pressure, enabling the Gibb's free energy of formation of $NiSO_4$(l) and the partial molar properties of the Na_2SO_4-$NiSO_4$ melt to be determined.

A. Experimental Procedure

A schematic diagram of the experimental apparatus is shown in Figure 2. A platinum crucible, containing a mixture of reagent grade Na_2SO_4 and NiO, was placed inside the mullite reaction tube in the furnace. The experimental gas mixtures consisted of air, SO_2, SO_3 and argon. To maintain the equilibrium concentration of SO_3, an air + SO_2 mixture, in the required proportions, was passed through a furnace containing disc-shaped honeycomb platinum catalysts, before entering the reaction furnace. The catalyst furnace was maintained at the same temperature as that of the reaction furnace. Another catalyst was placed just above the platinum crucible in the reaction furnace. All the connecting tubes were heated to 150°C, with heating tapes in order to avoid any SO_3 condensation. After the gas mixture had passed through the system for sufficient time, the platinum crucible, containing the oxide/Na_2SO_4 mixtures, and the catalyst assembly, was lowered into the hot zone of the furnace by means of the magnet and pulley assembly, as shown in Figure 2. This assembly also facilitated rapid removal of the crucible from the hot zone at the end of the experiments. The crucible containing the salt mixture was weighed before and after reaction with the gas mixture, the change in mass being used to determine the mass of $NiSO_4$ formed. In addition, the equilibrated salt mixture was dissolved in distilled water and analysed for Ni^{++} ion concentration by atomic absorption spectroscopy. The equilibration experiments were carried out until a constant mass was obtained. At 900°C, the time required for the attainment of equilibrium was about 6-8 hrs., correspondingly longer times were required at lower temperatures. All the experiments were carried out at SO_3 partial pressures below that required for the formation of $NiSO_4$ at unit activity. The equilibrium concentrations of SO_2 and SO_3 were calculated using thermodynamic data from Barin and Knacke (10).

Experiments were also carried out to investigate the possible formation of pyrosulfates, which would presumably affect the equilibrium measurements. However, there was no detectable mass change, when Na_2SO_4

alone was placed inside the reaction chamber, with the flowing air/SO_2/SO_3 mixture, thus indicating that within the SO_3 partial pressure range investigated, pyrosulfate formation was not responsible for any mass change.

B. Results and Discussion

The equilbrium $NiSO_4$ contents of the melt at various SO_3 partial pressures are shown in Table IV. All the compositions reported here are in the liquid region of the Na_2SO_4-$NiSO_4$ system. As given earlier, the activity of $NiSO_4$ in the melt can be described as

$$RT\ln a^L_{NiSO_4} = RT\ln \left\{ \frac{x^L_{MSO_4}}{1+x^L_{Na_2SO_4}} \right\} + \omega_L(1-x^L_{NiSO_4})^2 \quad (16)$$

The sulfation reaction for NiO can be written as

$$NiO(s) + SO_3(g) = \underline{NiSO_4}(l) \text{ (dissolved in } Na_2SO_4)(17)$$

and the free energy change for reaction (17) can be expressed as

$$-\Delta G^\circ_{(17)} = [RT\ln \left\{ \frac{x^L_{NiSO_4}}{1+x^L_{Na_2SO_4}} \right\} - RT\ln P_{SO_3}]$$

$$+ \omega_L(1-x^L_{NiSO_4})^2 \quad (18)$$

Thus, a plot of $[RT\ln (\frac{x^L_{NiSO_4}}{1+x^L_{Na_2SO_4}}) - RT\ln P_{SO_3}]$ versus $(1-x^L_{NiSO_4})^2$ should give a straight line. Figure 3 shows this relationship at three different temperatures. There appears to be an excellent agreement between the theory and experimental data in the concentration and temperature range investigated. The best straight line through the experimental points was obtained by a least squares method and Table V shows the $\Delta G^\circ_{(17)}$ and the interaction energy parameter values at three different temperatures.

According to Table V, an average value of ω_L = -5.21 kcal. $mole^{-1}$ is obtained. Using this value, and the single experimental points at other temperatures, $\Delta G^\circ_{(17)}$ at other temperatures can be obtained from eqn.(18). Figure 4 shows a plot of $\Delta G^\circ_{(17)}$ versus temperature which demonstrates a linear relationship in the temperature range 1100-1173K and which is given by the least squares expression.

$$\Delta G^\circ_{(17)} = -46095 + 36.954T \text{ cal.} \qquad (19)$$

in the temperature range 1100-1173K.

At the lower temperatures (1050 and 1023K), the concentration of $NiSO_4$ in the melt at the experimental SO_3 partial pressures used was relatively high (greater than 30 mole %), since at these temperatures the concentration of $NiSO_4$ at the liquidus is relatively high (for example at 1023 K, $x^L_{NiSO_4}$ is 0.25). Thus, under these conditions, the equilibration experiments can only be performed at high concentrations of $NiSO_4$ in the melt, when a concentration-independent, regular solution interaction parameter may not be a good approximation. As a consequence, at the lower temperatures, the equilibration experiments were restricted to one datum point only.

There are no direct measurements of the standard free energy change for reaction 17, which can be used for comparison with the present results. There are, however, data on the solubility of NiO in molten Na_2SO_4 at 1200K as a function of Na_2O activity in the dilute solution region (6), and these can be compared with the solubilities calculated from $\Delta G^\circ_{(17)}$ extrapolated to 1200K and the interaction energy parameter, ω_L, determined in the present work. The SO_3 partial pressure and Na_2O activity are related by the reaction:

$$Na_2SO_4(l) = Na_2O(l) + SO_3(g) \qquad (20)$$

$$K_{20} = \frac{a^L_{Na_2O} \cdot P_{SO_3}}{a^L_{Na_2SO_4}} \qquad (21)$$

Table VI compares the calculated solubilities of NiO in molten Na_2SO_4 at 1200 K, with those determined by Gupta and Rapp (6). There is reasonably good agreement between the two values within the limits of experimental uncertainties.

Assuming that the entropy of fusion for $NiSO_4$ in equal to 3 cal. K^{-1} g.ion^{-1} (see earlier), the enthalpy of fusion and the melting point of $NiSO_4$ can be estimated from the solubility measurements. Using the $\Delta G^\circ_{(17)}$ data at 1173K, and Kellogg's data (25) for the standard Gibb's free energy change for the reaction

$$NiO(s) + SO_3(g) = NiSO_4 \qquad (22)$$

ΔG°_{fusion} for $NiSO_4$ at 1173K is calculated to be 801 cal mol.$^{-1}$ Thus, assuming a temperature-independent entropy and enthalpy of fusion, the melting point and the enthalpy of fusion are estimated to be 1306K and 7.84 kcal. mole^{-1} respectively. Since the error introduced in the magnitude of ΔG°_{fusion} by the assumption of a temperature-independent entropy and enthalpy of fusion, is negligible at temperatures close to the melting point, the ΔG°_{fusion} value for the highest experimental temperature (1173K) was utilized to estimate the enthalpy and entropy of fusion of $NiSO_4$.

6. APPLICATION TO HOT CORROSION

The relevance of the solubility of NiO and Co_3O_4 in molten Na_2SO_4 to the hot corrosion process above the melting point of Na_2SO_4, and the corresponding stability diagrams for the Na-Ni-S-O and Na-Co-S-O systems has been discussed by Gupta and Rapp (6) and need not be elaborated here. However, the thermodynamic properties of binary Na_2SO_4-$NiSO_4$ and Na_2SO_4-$CoSO_4$ melts are of even greater significance in the low temperature hot corrosion process, since the formation of molten mixed sulfates is a necessary pre-requisite for the corrosion to initiate.

In the absence of any other thermodynamic information for the Na_2SO_4-$NiSO_4$ system, the present data in the temperature range 1100-1173°K can be tentatively extrapolated to other temperatures, and used to predict the minimum SO_3 partial pressure in the atmosphere necessary for liquid formation at different temperatures. The liquidus composition can be obtained from the Na_2SO_4-$NiSO_4$ phase diagram (12) and, using the ω_L value obtained in the present study, the minimum SO_3 partial pressure necessary for liquid formation calculated from eqn.(18). The results for the Na_2SO_4-$NiSO_4$ system are presented in Figure 5, which is essentially a stability diagram similar to that of Luthra and Shores (4, 5) for the Na_2SO_4-$CoSO_4$ system.

The minimum P_{SO_3} for liquid formation rises from a value of about 3×10^{-4} atm. at 700°C to a maximum of about 8×10^{-4} atm. at 800°C, decreasing again at higher temperatures. Essentially, there are two opposing factors: firstly, the minimum $NiSO_4$ content for liquid formation decreases with increasing temperature, but secondly the stability of $NiSO_4$ at a given P_{SO_3} in the atmosphere also decreases with increasing temperature. Jones (3) has measured the minimum $SO_2 + SO_3$ concentration in the gas necessary for liquid sulfate formation at 991K; his value of approximately 1000 ppm ($SO_2 + SO_3$) is in good agreement with Figure 5.

For the Na_2SO_4-$CoSO_4$ system, the sulfation reaction for the formation of $\underline{CoSO_4}(l)$, dissolved in Na_2SO_4, can be written as

$$1/3Co_3O_4(s) + SO_3(g) = \underline{CoSO_4}(l) + 1/6O_2(g) \qquad (23)$$

under conditions where Co_3O_4 is the stable oxide, and

$$CoO(s) + SO_3(g) = \underline{CoSO_4}(l) \qquad (24)$$

where CoO is the stable oxide. Using the melting point and enthalpy of fusion for $CoSO_4$ given earlier, and the interaction parameter for the liquid sulfate melt calculated from the phase diagram, the equilibrium partial pressure of SO_3 for a given concentration of $CoSO_4$ in the melt can be calculated. Figure 6 shows these values at the liquidus composition on the Na_2SO_4-rich side of the Na_2SO_4-$CoSO_4$ phase diagram. Since the equilibrium SO_3 partial pressure for reactions involving Co_3O_4 is inversely proportional to $P_{O_2}^{1/6}$, the results are shown for two different oxygen partial pressures, 0.21(air) and 0.021 atm. The line for the CoO reaction is also shown.

Several gas equilibration experiments, similar to those for the Na_2SO_4-$NiSO_4$ system, were carried out, and the measured solubilities of Co_3O_4 at three different temperatures are compared with calculated values in Table VII. The agreement is acceptable at 1173K, but at lower temperatures, 1123 and 1073K, where there is appreciably higher concentrations of $CoSO_4$ in the liquid sulfate at the experimental SO_3 partial pressures, the calculated solubilities are considerably greater than the measured values. It seems, therefore, that at higher solute concentrations, the simple regular solution model may not be a very good approximation. Nevertheless, the simplicity of the model justifies its use, since the basic purpose of the present analysis is to predict an order of magnitude of P_{SO_3} necessary for liquid formation. Measurements by Jones (3) indicate a value of 200 ppm (SO_2 + SO_3) at 991 K, which is consistent with the present analysis.

Figure 6 also compares the P_{SO_3} necessary for liquid formation calculated in the present study with that calculated by Luthra and Shores (5). The values in the present study are some 3-4 times higher, and these differences are presumably related to (a) the use of a higher value for the entropy of fusion of $CoSO_4$(see earlier) and (b) the use of the Temkin ionic model instead of the molecular model used in the earlier work (5). Luthra and Shores (4, 5) attempted to justify their calculated curve by oxidizing Co or CoO coupous in air or oxygen to produce a thin film of Co_3O_4 on the surface. These samples were then sprayed with 2.5 mg/cm^2 of Na_2SO_4 and exposed to O_2-SO_2-SO_3 environments for a few hours. The salt on the surface of the samples was then examined under a low power microscope for signs of melting. Liquid was observed at a P_{SO_3} of 5 x 10^{-5} atm. at 770°C. This value corresponds to the minimum P_{SO_3} calculated in the present work, for the formation of a liquid sulfate from CoO, and it is suggested that the oxygen activity between the Na_2SO_4 deposit is somewhat lower than its value in the bulk gas stream.

7. CONCLUDING REMARKS

As indicated in the Introduction, the formation of a molten sulfate is a necessary precursor to accelerated rates of oxidation or hot corrosion in this intermediate temperature regime (650-800°C): solid sulfate deposits are essentially innocuous. The formation of a liquid sulfate depends critically on the SO_3 partial pressure in the gas stream and it is clear from a comparision of Figures 5 and 6 that in Co-based systems the minimum P_{SO_3} required is almost an order of magnitude lower than in corresponding Ni-based systems, making Co-base alloys much more susceptible to this low temperature hot corrosion, as indeed observed in practice. Furthermore, in Co-base systems, the minimum P_{SO_3} also depends on the oxygen partial pressure and if the presence of the deposit effectively reduces the P_{O_2} at the deposit/oxide interface, Co-base alloys would be even more susceptible to hot corrosion. Indeed, Co_3O_4 is often found as precipitates in the outer part of the corrosion products after hot corrosion testing (5, 26), indicating that whilst the conditions at the salt/oxide interface were conducive to dissolution, where the salt contacted the bulk atmosphere, Co_3O_4 was re-precipitated.

Clearly, the formation of the liquid sulfate also depends on the relative proportions of CoO(or NiO) and Na_2SO_4. In this lower temperature range of 650-800°C the oxidation behavior of Co-and Ni-base resistant alloys, which at high temperature normally rely for their protection on the formation of a continuous layer of Al_2O_3 or Cr_2O_3, has not been well characterized. However, it is anticipated that formation of a continuous layer of the protective oxide will be difficult at least in the early stages of oxidation. Thus, formation of the base metal oxides NiO or CoO will continue for some appreciable time. What appears then to be important is the rate of formation of the CoO (or NiO) relative to the rate of Na_2SO_4 deposition, since this determines whether the surface deposit would pass through a composition regime containing the liquid phase. Higher concentrations of Na_2SO_4 would maintain the deposit in a solid form, although this would hardly recommend itself as a preventive measure.

8. ACKNOWLEDGEMENTS

This work was supported by the Director, Office of Energy Research, Office of Basic Energy Sciences, Materials Science Division of the U.S. Department of Energy under Contract Number W-7405-ENG-48.

REFERENCES

1. J. A. Goebel and F. S. Pettit, Metall. Trans. 1, 1943 (1970).

2. D. J. Wortman, R. E. Fryxell, and I. I. Bessen, Paper 11, presented at Third Conference on Gas Turbine Materials in a Marine Environment, Bath England, September 1976.

3. R. L. Jones, N. R. L. memorandum report 4409 (Nov. 1980).

4. D. A. Shores and K. L. Luthra, "Corrosion and Erosion Behavior of Materials," Proc. of Conf. of Met. Soc. AIME, ed. K. Natesan, p. 86 (1980).

5. K. L. Luthra and D. A. Shores, This Journal, 127, 2202 (1980).

6. D. K. Gupta and R. A. Rapp, This Journal, 127, 2194 (1980).

7. W. P. Stroud and R. A. Rapp, High Temperature Metal Halide Chemistry, edited by D. L. Hildenbrand, D. D. Cubicciotti, Electrochemical Society, p. 547 (1978).

8. W. W. Liang and J. F. Elliott, Properties of High Temperature Alloys, edited by Z. A. Fouroulis and F. S. Pettit, Electrochemical Society, p. 557 (1976).

9. J. Lumsden, "Thermodynamics of Molten Salt Mixtures," Academic Press (1966).

10. I. Barin and O. Knacke, "Thermochemical Properties of Inorganic Substances," Springer Verlag (1973-77)

11. T. Forland, J. Phys. Chem. 59, 152 (1955).

12.[+] K. A. Bolshakov and P. I. Fedorov, Zhur. Obshchei Khim., 26, 349 (1956).

13. S. K. Saxena, "Thermodynamics of Rock-Forming Crystalline Solutions," Springer-Verlag (1973).

14. K. K. Kelly, Bull. U. S. Bur. Mines, No. 393 (1936).

15.[+] G. Calcagani and D. Marotta, Atti reale Acad. Lincei, sez. II, 22, 375 (1913).

16.[+] A. Ballanca and M. Carapezza, Periodico Mineral (Rome) 20, 280 (1951).

17.[+] W. Grabmann, Z. anorg. Chem. 81, 272 (1913).

[+] In "Phase Diagrams for Ceramists," Ed. and publ. by the American Ceramic Society.

18.[+] V. E. Plyushchev and L. N. Komissarova, Dokl. Akad. Nank. SSSR 85 (5), 1042 (1952).

19.[+] W. Grabmann, Z. anorg. Chem. 81, 270 (1913).

20.[+] A. S. Ginsberg, Z. anorg. Chem. 61, 126 (1909).

21.[+] W. Grabmann, Z. anorg. Chem. 81, 295 (1913).

22.[+] C. Perrier and A. Bellanca, Periodica Mineral (Rome) 11, 189 (1940).

23.[+] W. Grabmann, Z. anorg. Chem. 81, 289 (1913).

24. O. Kubaschewski, E. L. Evans and C. B Alcock, "Metallurgical Thermochemistry," Pergamon Press (1967).

25. H. H. Kellogg, Trans. AIME 230, 1622 (1964).

26. A. K. Misra and D. P. Whittle, to be published.

[+]In "Phase Diagrams for Ceramists," Ed. and publ. by the American Ceramic Society.

TABLE I. Entropy of Fusion for Sulfates of MSO_4-Type (10)

	ΔS_{fusion} (cal. K^{-1} g. ion^{-1})
$CaSO_4$	2
$PbSO_4$	3.52
$BaSO_4$	2.98
$MgSO_4$	1.25

TABLE II. Calculated Interaction Parameter Values, ω_L, for Na_2SO_4-$CoSO_4$ Melts

Temperature, K	ω_L kcal. $Mole^{-1}$
873	- 5.9
923	- 9.3
973	- 7.4
1023	- 8.1
1073	- 5.5
1098	- 4.7
1125	- 3.2

TABLE III. Estimation of Enthalpies and Entropies of Fusion for Sulfates of the MSO_4-Type from the Phase Diagrams

System	Ref.	MSO_4	T_M,K	ΔH°_{fusion},kcal mole^{-1} (present estimate)	ΔH°_{fusion},kcal mole^{-1} (Kelley's(14)estimate)	ΔS°_{fusion}, cal.K^{-1} g. ion^{-1} (present estimate)
K_2SO_4-$CaSO_4$	17	$CaSO_4$	1735	11.8	6.7	3.41
Li_2SO_4-$CaSO_4$	18	$CaSO_4$	1723	8.3		2.39
K_2SO_4-$MgSO_4$	19	$MgSO_4$	1397	7.9	3.5	2.83
Na_2SO_4-$MgSO_4$	20	$MgSO_4$	1403	8.3		2.97
K_2SO_4-$PbSO_4$	21	$PbSO_4$	1353	10.6	9.6	3.93
Na_2SO_4-$PbSO_4$	22	$PbSO_4$	1350	10.3		3.82
K_2SO_4-$BaSO_4$	23	$BaSO_4$	1853	11.5	9.7	3.09
K_2SO_4-$CuSO_4$	16	$CuSO_4$	1044	5.9	-	2.83
Li_2SO_4-$CdSO_4$	15	$CdSO_4$	1273	7.5	-	2.94

TABLE IV. $NiSO_4$ Content of Na_2SO_4 Melt as a Function of SO_3 Partial Pressure

Temperature, K	P_{SO_3}, (atm.)	$x^L_{NiSO_4}$
1173	3.67×10^{-4}	0.02
	7.35×10^{-4}	0.037
	1.47×10^{-3}	0.068
	2.246×10^{-3}	0.092
	3.425×10^{-3}	0.123
	4.224×10^{-3}	0.136
	4.875×10^{-3}	0.154
	5.275×10^{-3}	0.157
1150	8.7×10^{-4}	0.052
	1.58×10^{-3}	0.084
	2.64×10^{-3}	0.117
	3.32×10^{-3}	0.133
	4.075×10^{-3}	0.152
	5.025×10^{-3}	0.173
	5.826×10^{-3}	0.187
	6.275×10^{-3}	0.196
1123	3.42×10^{-3}	0.172
	4.129×10^{-3}	0.192
	4.975×10^{-3}	0.213
	6.175×10^{-3}	0.237
	7.125×10^{-3}	0.257
	7.72×10^{-3}	0.266
1100	2.37×10^{-3}	0.224
1050	3.63×10^{-3}	0.307
1000	4.77×10^{-3}	0.38

TABLE V. Interaction Parameter for Na_2SO_4-$NiSO_4$ Melts and the Free Energy of Formation of $NiSO_4(l)$

Temperature, K	ω_L, kcal. mole^{-1}	$\Delta G^\circ_{(17)}$, kcal. mole^{-1}
1123	-5.13	-4.25
1150	-5.26	-3.43
1173	-5.25	-2.75

TABLE VI. Comparison of Calculated and Measured Solubilities of NiO in Molten Na_2SO_4 at 1200 K

$-\log a^L_{Na_2O}$	P_{SO_3}, atm.	$x^L_{NiSO_4}$, measured(6)	$x^L_{NiSO_4}$, calculated
14.5	3.52×10^{-3}	0.103	0.087
11.6	4.43×10^{-6}	0.000251	0.00026

TABLE VII. Comparison of Experimental and Predicted Solubilities of Co_3O_4 in Na_2SO_4

Temperature, K	P_{SO_3}, atm.	$x^L_{CoSO_4}$, measured	$x^L_{CoSO_4}$, calculated
1073	2.5×10^{-3}	0.427	0.503
1123	7.73×10^{-3}	0.432	0.576
	7.35×10^{-4}	0.272	0.207
1173	1.47×10^{-3}	0.374	0.321

FIGURE CAPTIONS

Figure 1. The Na_2SO_4-$CoSO_4$ phase diagram (12).

Figure 2. Schematic diagram of the gas equilibration apparatus.

Figure 3. Verification of regular solution behavior for Na_2SO_4-$NiSO_4$ melts.

Figure 4. Standard free energy of formation of $NiSO_4(l)$ as a function of temperature.

Figure 5. Minimum P_{SO_3} required for liquid sulfate formation as a function of temperature in the Na_2SO_4-NiO-SO_3 system.

Figure 6. Minimum P_{SO_3} required for liquid sulfate formation as a function of temperature in the Na_2SO_4-$CoO(Co_3O_4)$-SO_3 system.

Na_2SO_4–$CoSO_4$

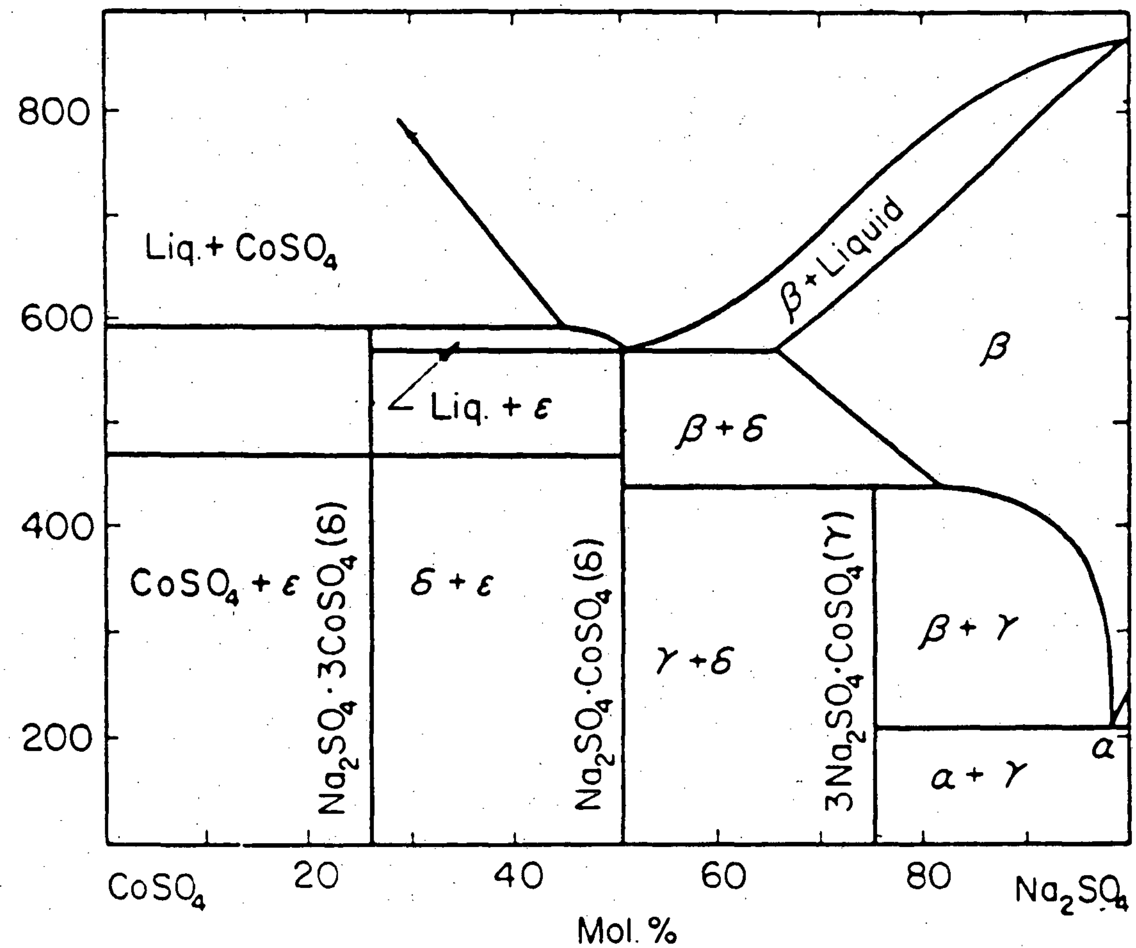

XBL 809-11583

Figure 1.

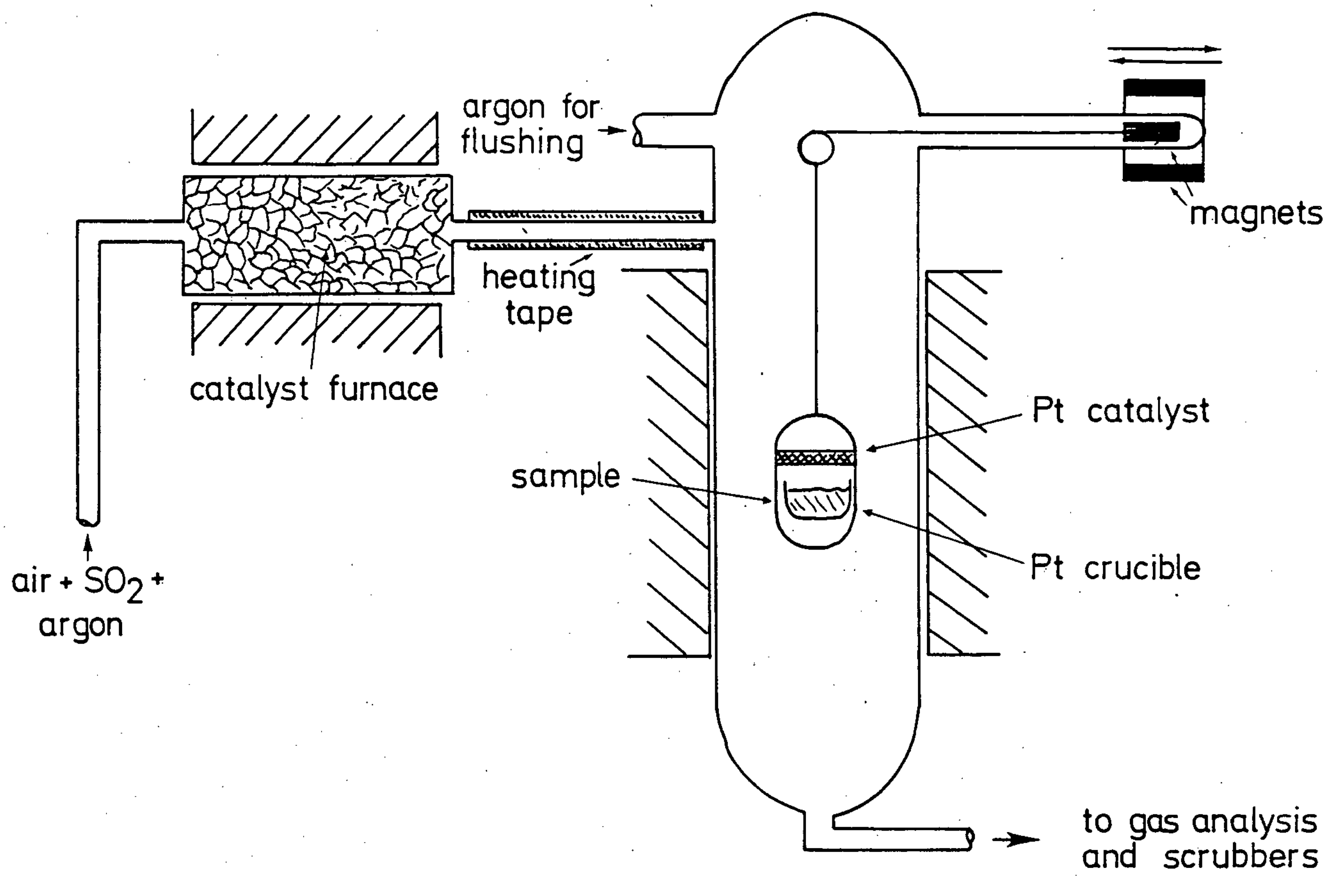
argon for flushing
magnets
heating tape
catalyst furnace
Pt catalyst
sample
Pt crucible
air + SO_2 + argon
to gas analysis and scrubbers
XBL 8110-11904

Figure 2.

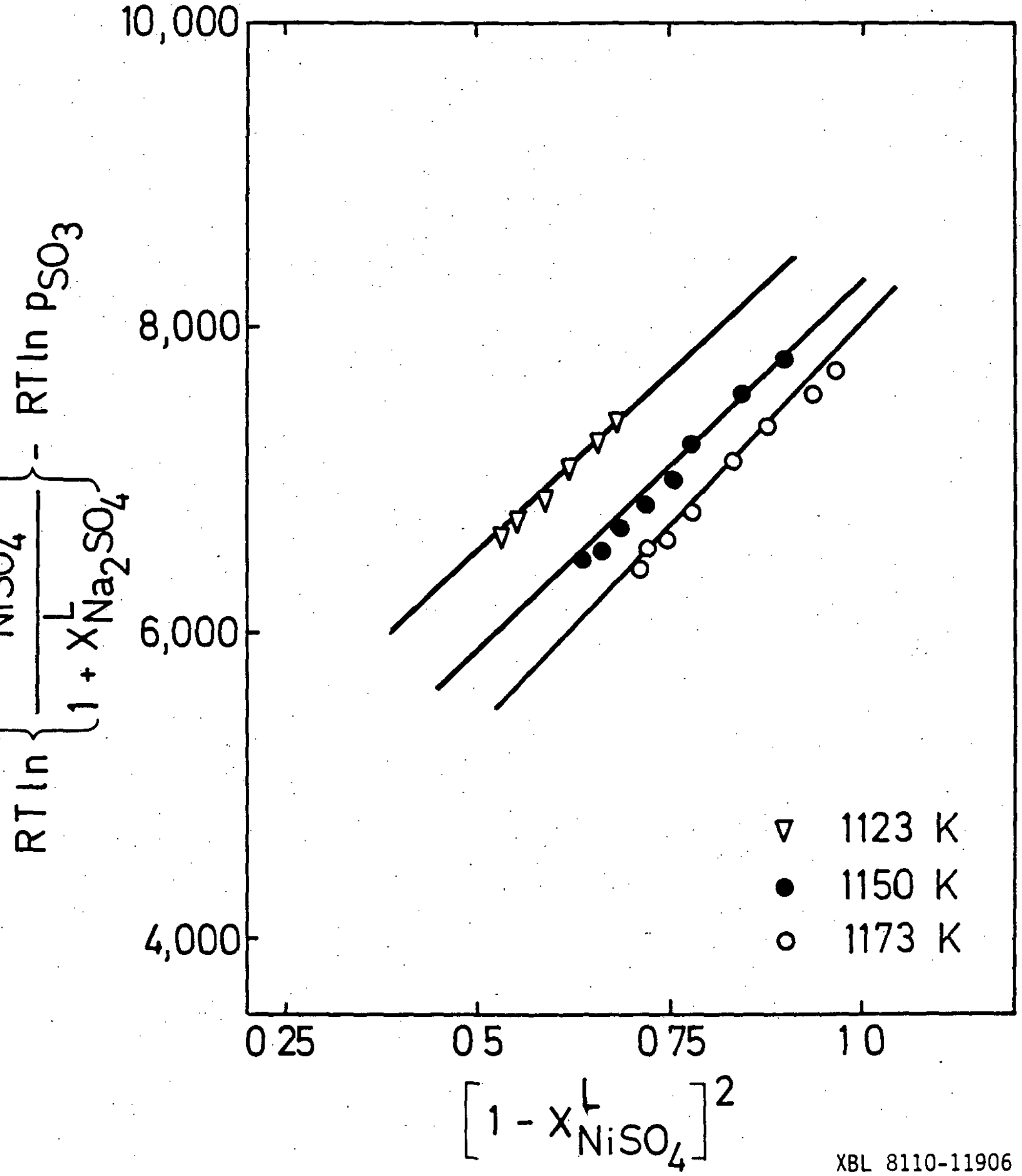
10,000
8,000
6,000
4,000
0.25
0.5
0.75
1.0
RT ln { X^L NiSO4 / (1 + X^L Na2SO4) } - RT ln pSO3
[1 - X^L NiSO4]^2
▽ 1123 K
● 1150 K
○ 1173 K
XBL 8110-11906

Figure 3.

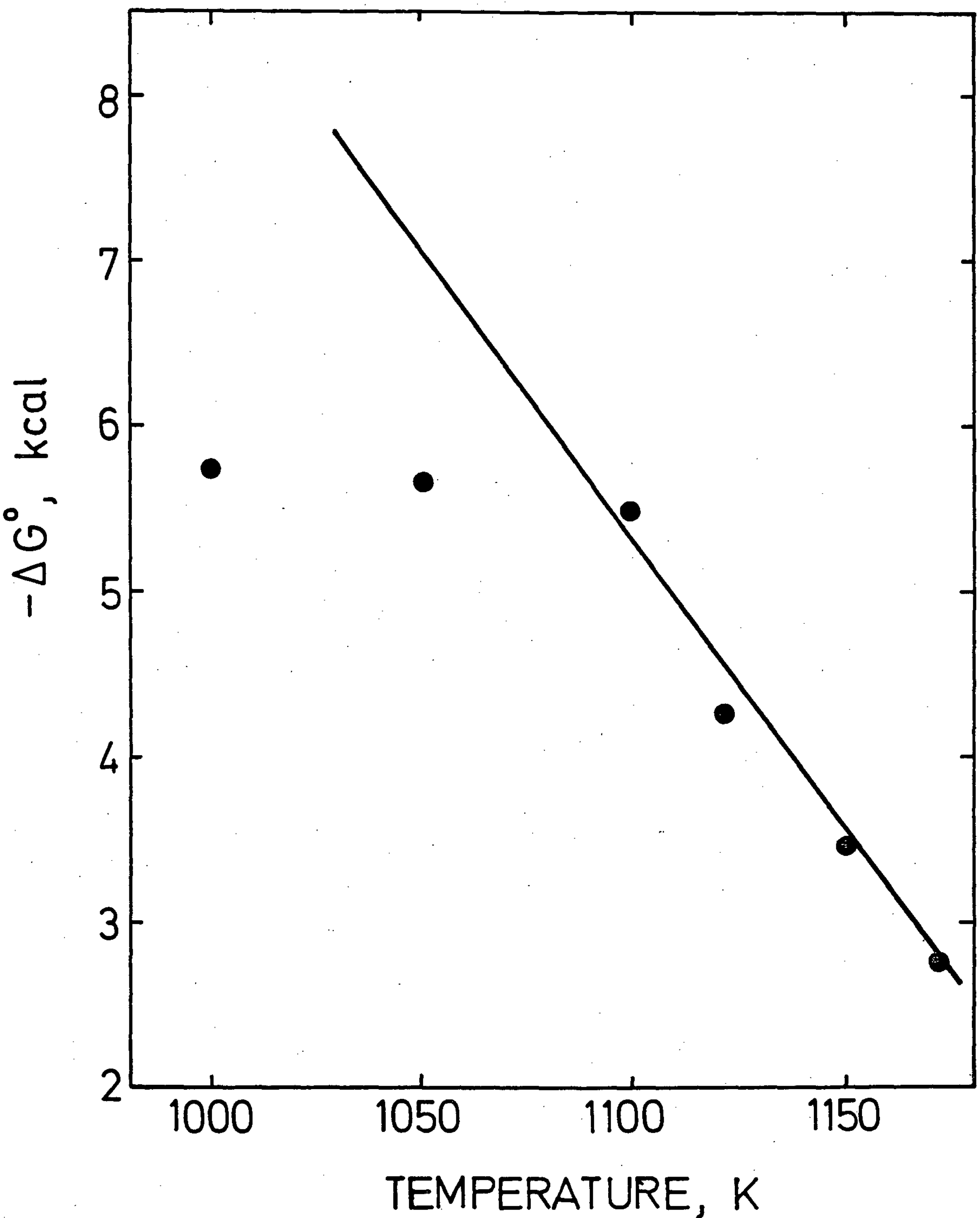

Figure 4.

XBL 8110-11905

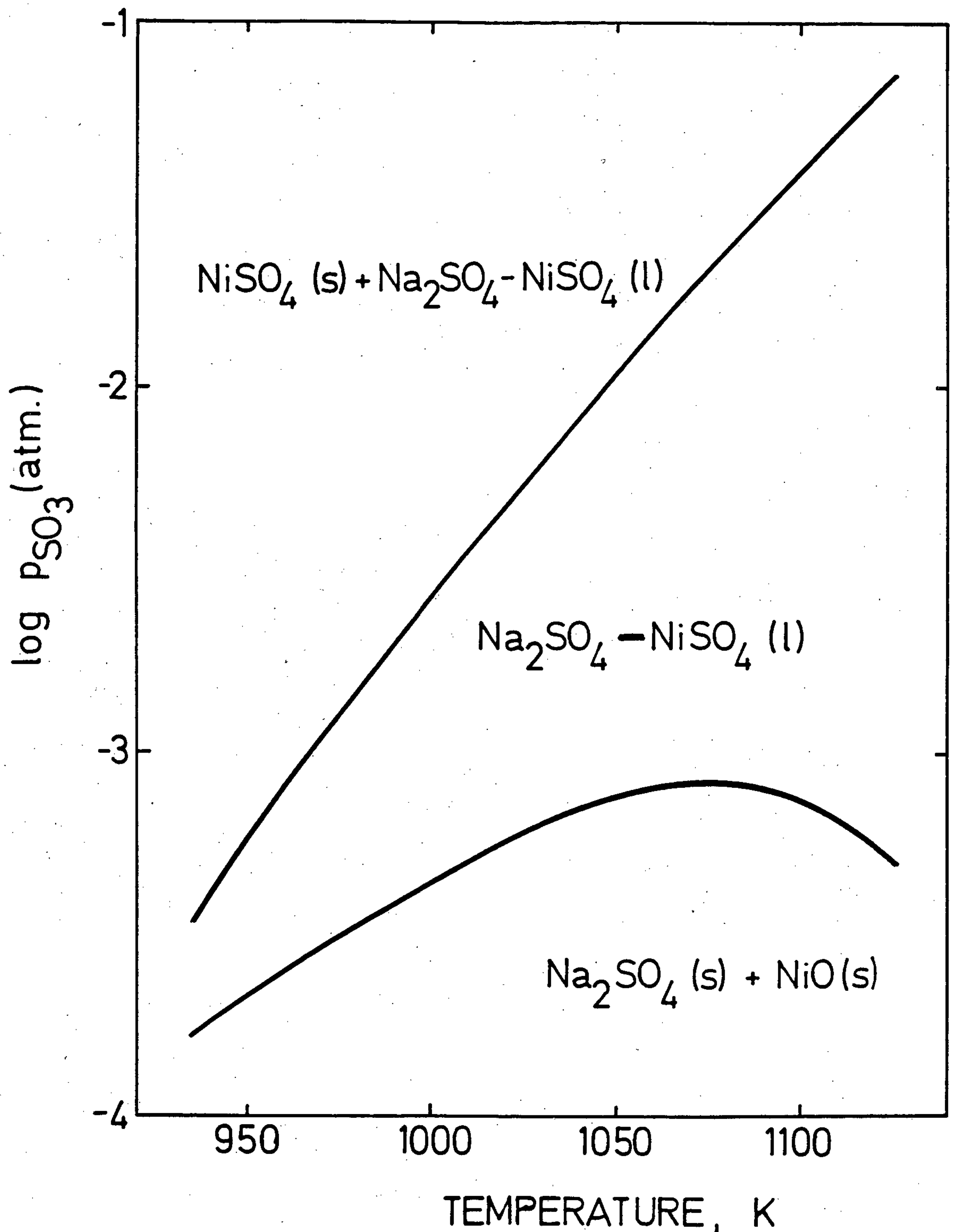

Figure 5.

XBL 8110-11902

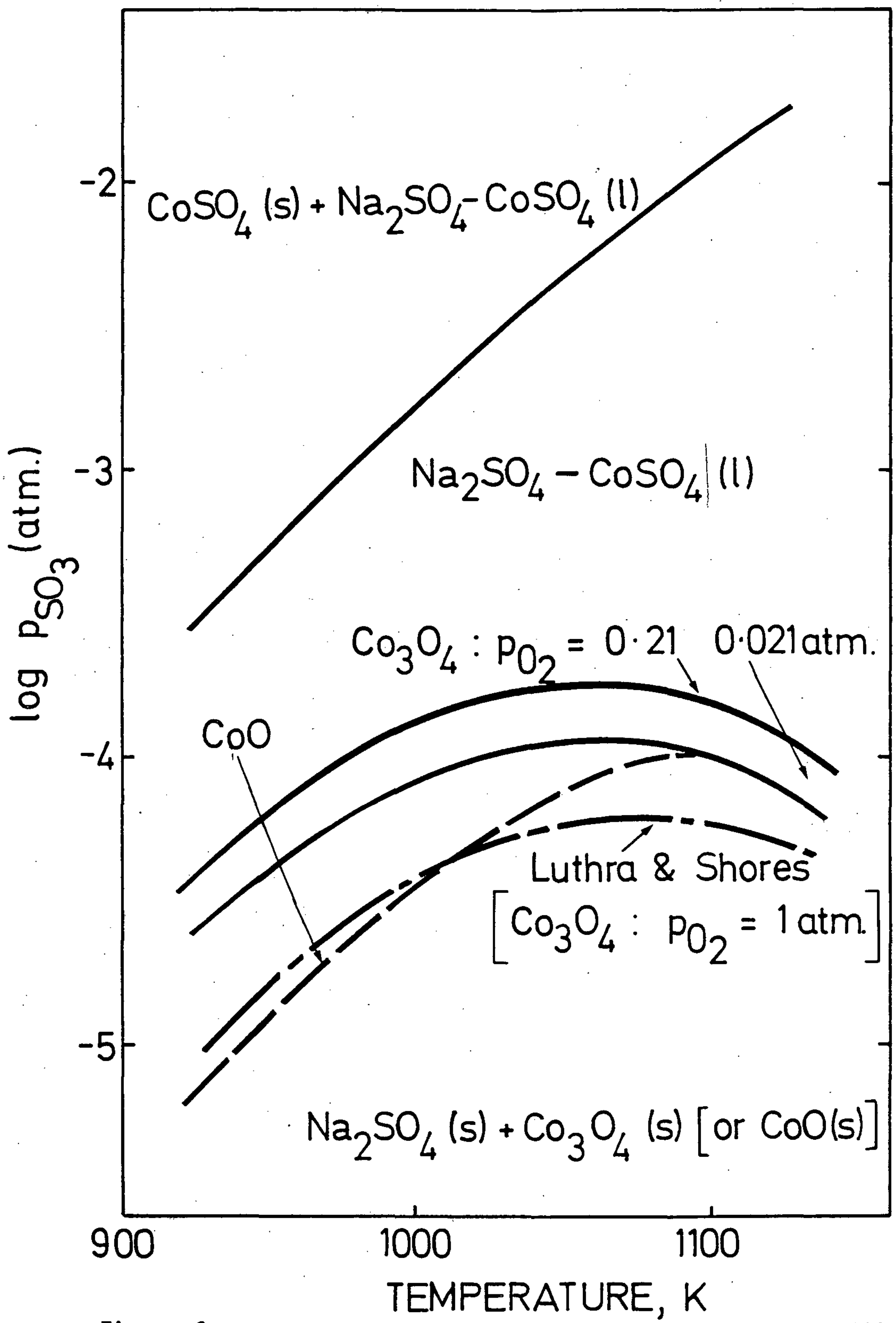

Figure 6.

XBL 8110-11903

TECHNICAL INFORMATION DEPARTMENT
LAWRENCE BERKELEY LABORATORY
UNIVERSITY OF CALIFORNIA
BERKELEY, CALIFORNIA 94720